4.3.2.2 Secondary Nuclei

We have examined the *HST* images for evidence of any secondary nuclei, as was suggested by Sekanina (1998b). We deconvolved the residual images left after our application of the coma-fitting method. We used the same point-spread function as Sekanina used, and also a theoretical one that we found to closely mimic the structure of observed stars. The two PSFs differ a bit in shape, but are not too dissimilar when pixelized to the WFPC2 PC resolution. We found no clear indication of a second nucleus; we were able to obtain satisfactory fits to our residual maps using just one point-source. A second point-source would of course improve our fits but not significantly. Moreover we do not find the need to introduce a secondary nucleus as strong (about one-fifth the brightness of the primary) as mentioned by Sekanina (1998b). Undoubtably this is due to the different methods used to model the emission from the coma; Sekanina uses an analytic function with just a few parameters to match the coma's brightness whereas we are fitting the structure at every azimuth for a total of a few hundred parameters. It is also possible that the secondary nuclei that Sekanina claims are actually jet features in the near-nuclear coma.

4.3.2.3 Microwave

We detected the thermal continuum from the comet's nucleus at the $7-\sigma$ level after a 66-hr integration at VLA. The image is a point source, and the most important section of our CLEAN map is shown in Fig. 4.14. The detection at VLA of Hale-Bopp's thermal continuum was the first such detection by that observatory, after only upper-limits were found for five other comets (Snyder *et al.* 1983, de Pater *et al.* 1985, Schenewerk *et al.* 1986, Hoban and Baum 1987, and Chapter 6 of this thesis). It is arguably the first detection ever of the thermal continuum radiation from a cometary nucleus in the centimeter-regime; similar observations of comets West (C/1975 XX = 1976 XX = 1975n; Hobbs *et al.* 1977) and Kohoutek (C/1973 XX = 1973 XX = 1973f; Hobbs *et al.* 1975) imaged their comae, and single-dish observations of comet *IRAS*-Araki-Alcock (Altenhoff *et al.* 1983), while yielding fluxes consistent with a nucleus, had beam sizes that were large enough to arguably include flux from the coma, especially since a skirt of decimetersized grains was detected by the radar experiments of Goldstein *et al.* (1984) and Harmon *et al.* (1989). Our VLA measurements had a synthesized HPBW of only 1 arcsecond, and moreover a reduction of the data excluding the very long antenna baselines of VLA, which de-emphasizes any smooth underlying component to the emission (i.e., a coma), still yielded a point source. Hence, we conclude that thermal emission from centimeter-to-decimeter sized grains in Hale-Bopp's coma is negligible in comparison to the emission from the nucleus itself. At the very least, this is the first interferometric detection of the microwave continuum from a nucleus.

There have been other interferometric observations of the radio continuum, in the millimeter regime, and they too were taken near perihelion, so we can construct a radio spectrum of the Hale-Bopp nucleus, one of the first such spectra in existence. This is shown in Fig. 4.15. We used the fluxes reported by Altenhoff *et al.* (1999) using the IRAM Plateau de Bure interferometer, and Blake *et al.* (1999) using the

Owens Valley interferometer, and scaled them to account for the small differences in geocentric distance in the comet. The spectrum follows the λ^{-2} RayleighJeans law quite well; fitting the points to a line implies the emissivity could not have any more than a $\lambda^{-0.1}$ overall dependence. Alternatively, the deviation from the Rayleigh-Jeans law could be due to the different depths (and hence different temperatures) at which the millimeter-wave and centimeter-wave observations sample.

4.3.3 Discussion

4.3.3.1 Model of Microwave Emission

Use of the augmented thermal model I described in Chapter 3 is justified with comet Hale-Bopp, since we have an idea of the rotation state and photometry at multiple wavelengths. The extra trick however is that the microwave data does not sample the nucleus' surface but several (radiative) skin depths deep, and the flux that the augmented model predicts for the centimeter wavelengths depends on how steep the temperature gradient is within the nucleus. The wavelength is 3.55 cm; exactly how far down from the surface the continuum is emitted is a matter of some debate, it could be a few wavelengths – roughly one decimeter – if the material is mostly rock, or it could be significantly larger, roughly half a meter or more, if a substantial ice component is present (de Pater *et al.* 1985). Since the cometary ice is not expected to be found in patches around the surface but rather in a mixture with the rock, I will choose the former scenario to constrain the modeling.

Another matter that one must take into account is the effect of the coma on the total energy put into the nucleus. The contribution of direct sunlight is decreased due to the optically thick coma, but this is somewhat compensated by the thermal emission of the dust and, to a lesser extent, by the scattering of the visual-band sunlight off the dust grains. Salo (1988) has already made detailed calculations of the energy available to a nucleus surrounded by a coma of a given optical depth with grains of a given single-scattering albedo and Henyey-Greenstein asymmetry factor (Henyey and Greenstein 1941). I will use his results here. For small (1 micron and below) dust grains, of which Hale-Bopp was a prodigious producer (Lisse *et al.* 1999a, Williams *et al.* 1997), forward scattering is expected to be important, and Salo (1988) calculates that in that case the reradiative component to the total power onto the nucleus would be about 50 to 60% of the total power on a bare-nucleus. This is for opacities of unity and greater. In other words, in the limit of an infinitely thick coma, the nucleus would receive 50 to 60% of the energy it otherwise would without that coma. For the opacities of Hale-Bopp's coma, described in section 4.2, there would be the $e^{-\tau}$-reduced direct sunlight component also, or 30 to 40% of the unextincted sunlight, to bring the total to about 80 to 90% of the original available energy. I do not want to overstate the accuracy of this calculation; other workers have done similar computational experiments and have found different answers depending on the model assumptions (e.g. Marconi and Mendis 1984, Hellmich 1981). However the consensus seems to have the nucleus losing little net available energy despite having a coma with $\tau \approx 1$.

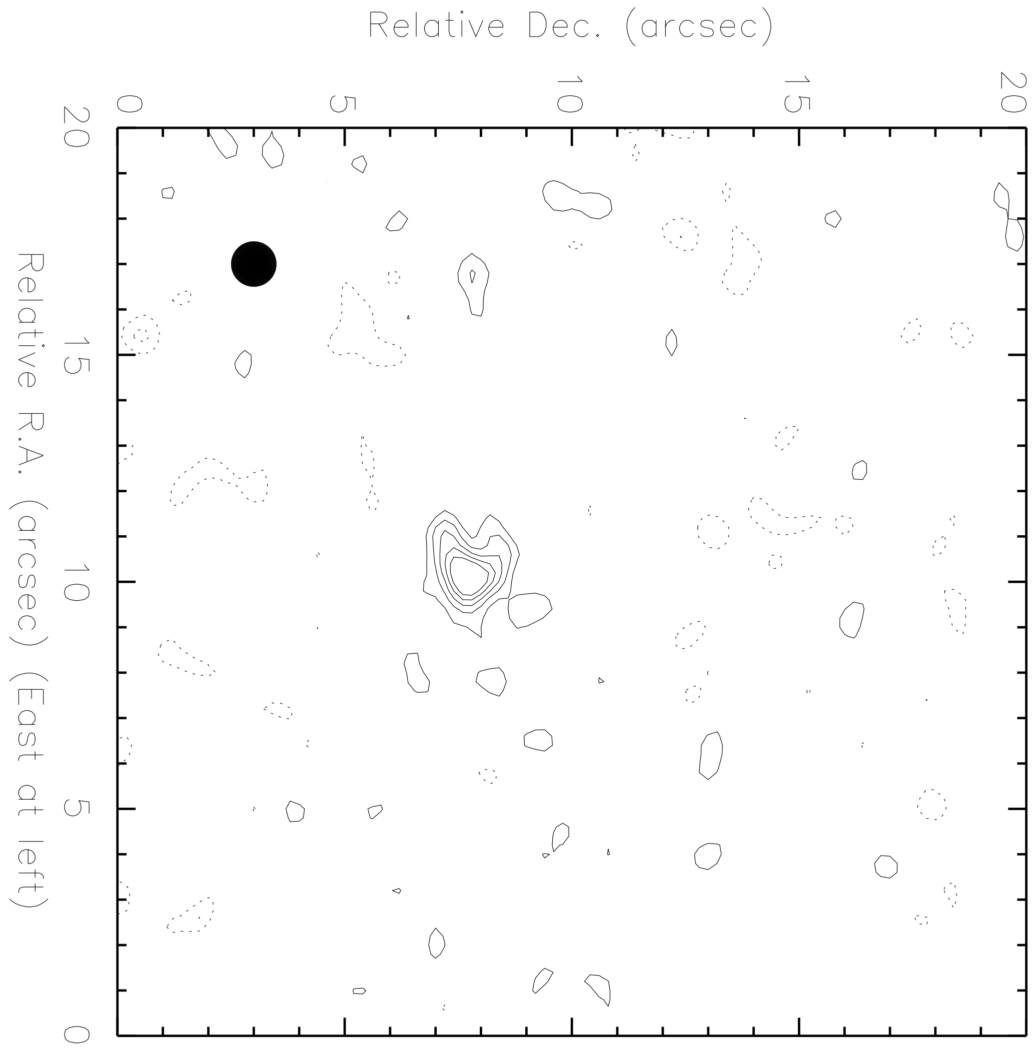

Figure 4.14: CLEAN contour map of comet Hale-Bopp microwave continuum. This the image obtained with the VLA, between 20 and 27 March 1997, of the nucleus' microwave continuum. The CLEAN algorithm has been applied. Contours are -2, 2, 3, 4, 5, and 6 σ. The dark circle at lower left represents the synthesized beam HPBW, about 1 arcsec wide.

Thus, the augmented model was modified to allow an additional 50% of the solar flux on top of the extincted ($\sim e^{-1}$) direct contribution. The rotation period of 11.3 hr was used, and the comet's rotation axis was directed toward a cometocentric ecliptic longitude of 275° and latitude of −50°, a direction close to what has been derived by several groups (Licandro *et al.* 1999, Jorda *et al.* 1999). The shape of the nucleus is totally unknown, but due to its apparently large size it may be tempting to think of it as spherical. This is complete guesswork, since plenty of comparably-sized asteroids are elongated. To reduce the number of parameters I have arbitrarily set one axial ratio to 1.3 and the other to 1.0.

To model the microwave flux, I allowed the thermal inertia and effective radius to vary, leaving the opacity at unity. The problem was then to just find a combination of effective radius and emitting layer depth that produced the observed microwave flux. The trend is for the emitting layer to be deeper as both the effective radius and thermal inertia increase; a higher thermal inertia means there is less of a temperature gradient in the nucleus, and a higher effective radius simply means there is more surface area and the object is more luminous.

For a lunar-like thermal inertia, and an effective radius of 27 km, I find that my augmented model reproduces the observed flux if the microwave continuum were emitted from a layer 20 cm deep. This is toward the high end of the plausible depths – it is 6 wavelengths. For comparison, the thermal inertia for (3200) Phaethon (a likely dormant comet) is about 10 times the lunar value (Harris *et al.* 1998) and the emitting layer on Hale-Bopp would be about 120 cm deep, probably too far. However if the radius were in this case only about 19 km, then the emitting layer would be only 20 cm.

For a thermal inertia more like that of the Main Belt asteroids – roughly one-fifth the lunar value (Spencer *et al.* 1989) – the depth of the emitting layer is only 6 cm for a radius of 27 km, and so the radius can be very large, 50 km or more, if we allow the emitting layer to be as deep as 20 cm. Based on my occultation results, such a radius is too large since the impact parameter of that observation was so small, so one could conclude that Hale-Bopp's nucleus has lunar-like or Phaethon-like thermal inertia and the radius is in the 20 to 30 km range.

Figure 4.16a shows the temperature map derived from the augmented thermal model using the lunar-like thermal inertia. The axes are longitude and latitude. Since the nucleus is aspherical, the longitude and latitude system are based on the sphere that inscribes the ellipsoid; i.e., a sphere with a radius equal to the smallest semimajor axis of the ellipsoid. The undulations in the contours give some indication of where the elongation of the nucleus lies. Also note that near perihelion the currently accepted pole position pointed almost directly at the Sun, causing the almost STM-like contours. The flat temperature on the night side is due to the (isotropic) coma's contribution to the impinging power. Figure 4.16b shows the temperature map of the surface; the difference is about 150 K in just a few decimeters.

Of course near perihelion the nucleus' orientation with respect to the Sun was changing most rapidly. Depending on the inertia, this affects the model temperature map, especially since a large fraction of the Sun-facing hemisphere of the nucleus near perihelion is almost totally in darkness for most of Hale-Bopp's orbit. That

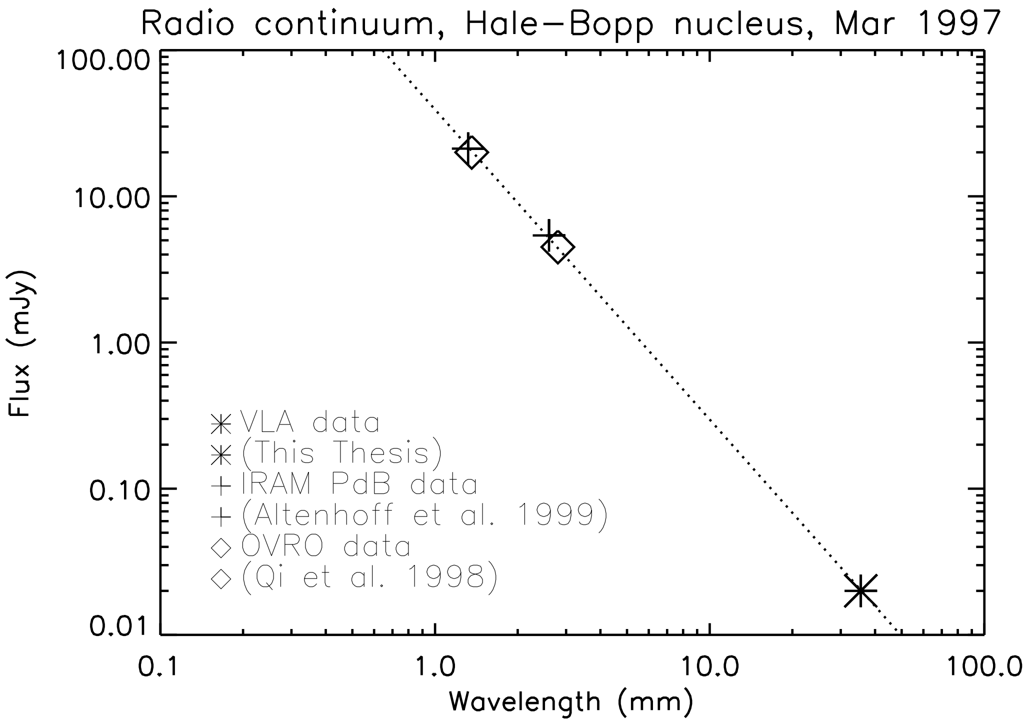

Figure 4.15: Radio continuum spectrum, Hale-Bopp nucleus. This broadband spectrum has been created by combining my VLA results with OVRO and IRAM PdB data. The points follow a Rayleigh-Jeans law quite well (dashed line). What little deviation there is could be due to wavelength dependence of the emissivity or the thermal gradient of the nucleus sampled by the different wavelengths.

hemisphere turns toward the Sun just a few months before perihelion and turns away again a few months after. For this reason, I ran my augmented thermal model over 50 to 60 rotations to remove any transient effects from the choice of initial conditions.

4.3.3.2 Model of Mid-IR Emission

The next step is to check the low conductivity and the effective radius with the infrared photometry from October/November 1996. Of course the coma's conditions are different but we will take the opacity to be approximately unity again. Unfortunately the model predicts about 2 Jy, less than half the 5 Jy we found from Fig. 4.12. In fact the radiation of thermal continuum from the dust would have to deliver about 200% of the energy received by a bare nucleus, not the 50% we have used, based on the work of Salo (1988). Under the formalism I have used here, the dust grains cannot be efficient enough to backwarm the nucleus surface to the requisite temperature. Now the grains of the coma were apparently indeed superheated (Williams *et al.* 1997, Lisse *et al.* 1999a), but this likely could not provide the extra energy needed since the emissivity of the grains is too low; these grains are smaller than the wavelength of the continuum emission spectrum's maximum.

Comet Hale-Bopp was about 3 AU from Earth at the time of these mid-IR observations, and so one pixel of the detector covered more than 700 km. Though it is a testament to the incredible infrared brightness of this comet, this pixel scale is much larger than the usual case, where we concentrate on comets that are less than 1 AU away. This means that the coma-to-nucleus brightness ratio within the central pixels is in general higher, since each of those pixels can pick up such a huge area of comatic flux. Thus, it is not completely surprising that the coma-fitting technique is unable to cleanly separate the coma and the nucleus. This "extra" point-source emission that the technique found in Fig. 4.12 may be related to the opacity of the coma near the nucleus.

4.3.3.3 Implications of Optical Measurements

The optical magnitudes of the nucleus in Table 4.5 can be used with above derived range of the radius to find the albedo. As stated, I will use the October 1995 value since that dataset is probably the least contaminated with an optically thick coma. Also note that the phase angle is small so there is little added error from the uncertain optical phase behavior. A caveat to this analysis is that different workers have derived different brightnesses for the embedded point source within these very same *HST* images (Weaver *et al.* 1997, Weaver and Lamy 1999, Sekanina 1999) using different, independent programs to account for the coma. This is almost certainly due to two factors: the pixel scale covers a large linear distance at the comet compared to the size of the nucleus, and the dust coma morphology in the inner coma is more complicated than what we naively see in the images. Small, subpixel features in the coma will adversely affect one's ability to photometrically extract the nucleus, especially when the comet is very active and nearly 3 AU away.

Yet another potential problem that adds to the error in the nuclear flux estimate is the unknown rotational context of the *HST* images, since we may be viewing different cross sections at different times.

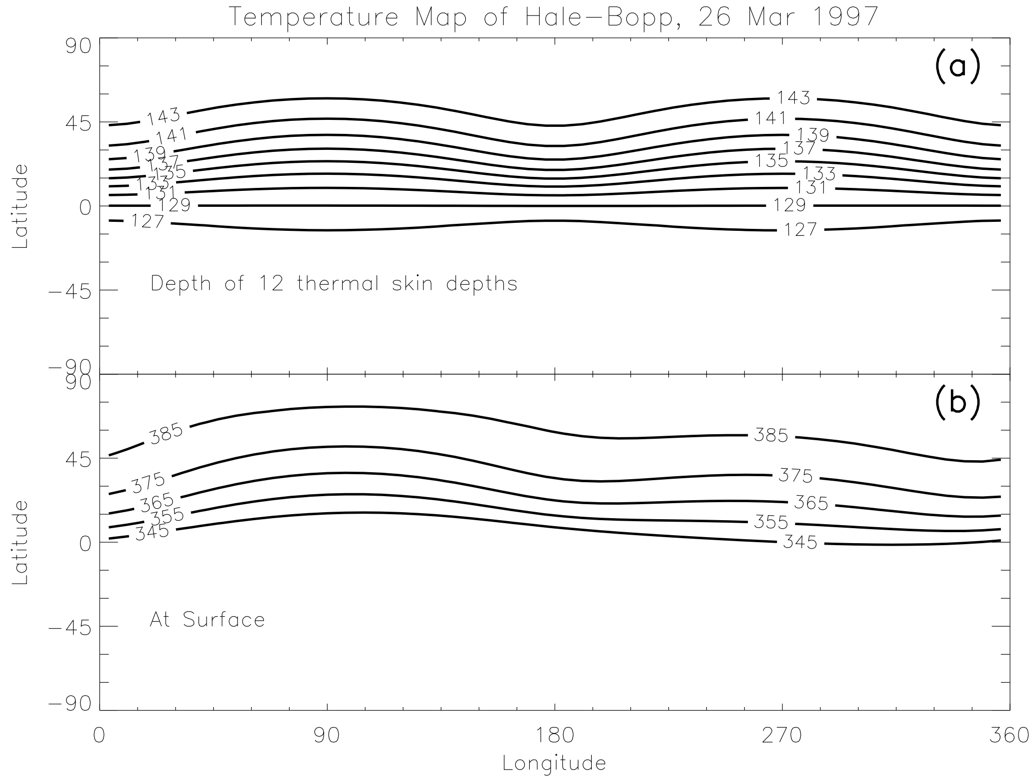

Figure 4.16: Temperature map of Hale-Bopp, 26 Mar 1997. This figure shows the temperature map of comet Hale-Bopp's nucleus for Mar 26 1997, during the time of our VLA microwave observations. The map was created from my augmented thermal model. The top panel shows the temperature 12 skin depths into the nucleus; the bottom shows the surface temperature. The temperature drops by roughly 150 K in just a few decimeters.

For an effective radius of 25 ± 5 km, and an *HST* R_C magnitude of 18.3 ± 0.1 on 23 Oct 1995, the geometric albedo is 6%±2%. Including the relatively dimmer nucleus found by Weaver *et al.* (1997) and Weaver and Lamy (1999), and the relatively brighter nucleus found by Sekanina (1999), the geometric albedo is within 4.5%±3%.

4.4 Summary of Hale-Bopp Results

The combination of the occultation observations and the modeling of the thermal data provides the following conclusions about Hale-Bopp's nucleus:

• If the thermal inertia to Hale-Bopp's nucleus is lunar-like or Phaethon-like, and if the emitting layer sampled by the VLA observations is less than 20 cm, then the effective radius of Hale-Bopp's nucleus is 25 ± 5 km. In general, the higher the thermal inertia, the smaller the radius must be in the range given. This range is also consistent with the upper limit derived from the occultation results, which set a limit of 30 km on the radius.

• These inertias and radii cannot reproduce the 5 ± 0.5 Jy of flux that was measured at 11 microns in October and November 1996, so presumably the large geocentric distance prevented our coma-fitting method from reliably extracting the nucleus. This is because there were too many kilometers at the comet per pixel, and hence too much coma.

• The occultation modeling assumed a spherical nucleus, so if the real nucleus deviates from this, then it is conceivable that the effective radius is larger than 30 km but that the section sampled during the occultation has locally a smaller radius, or that the near-nuclear dust coma has an unusual morphology that would fool us into thinking that the nucleus' radius is smaller than it is. In that case, the thermal inertia could conceivably be lower than the lunar value. Moreover, then it is easier to reproduce the thermal IR measurement from later 1996, since with a larger radius the nucleus has a higher luminosity.

• The optical *HST* data have been analyzed by many people in an attempt to extract the nuclear flux. Based solely on my results, the geometric albedo is 0.06 ± 0.02, but by including the efforts of others on the same dataset, the visual geometric albedo is 0.04 ± 0.035.

• Using the morphological changes in the mid-IR data, I constrain the rotation rate to be 11.3 hr $\pm$ 0.05 hr. Strictly speaking, this is the average rate between 4 and 12 April 1997.

Lastly, I mention the very significant finding of an optically thick inner coma from the occultation observation. This was the first time a dust coma with such a high opacity had been found.